

# Aging of poly(lactide)/poly(ethylene glycol) blends. Part 1. Poly(lactide) with low stereoregularity

Y. Hu<sup>a</sup>, M. Rogunova<sup>a,1</sup>, V. Topolkaraev<sup>b</sup>, A. Hiltner<sup>a,\*</sup>, E. Baer<sup>a</sup>

<sup>a</sup>Department of Macromolecular Science and Center for Applied Polymer Research, Case Western Reserve University, Cleveland, OH 44106-7202, USA

<sup>b</sup>Kimberly-Clark Corporation, Neenah, WI 54956, USA

Received 18 March 2003; received in revised form 24 June 2003; accepted 30 June 2003

## Abstract

Poly(lactide) (PLA) is rapidly gaining interest as a biodegradable thermoplastic for general usage in degradable disposables. To improve mechanical properties, a PLA with low stereoregularity was blended with poly(ethylene glycol) (PEG). Blends with up to 30 wt% PEG were miscible at ambient temperature. Blending with PEG significantly decreased the  $T_g$ , decreased the modulus and increased the fracture strain of PLA. However, the PLA/PEG 70/30 blend became increasingly rigid over time at ambient conditions. The mechanism of aging primarily under ambient conditions of temperature and humidity was studied. Changes in mechanical properties, thermal transitions and solid state morphology were examined over time. Aging was caused by slow crystallization of PEG. Crystallization of PEG depleted the amorphous phase of PEG and gradually increased the  $T_g$ . As  $T_g$  approached the aging temperature, reduced molecular diffusivity slowed the crystallization rate dramatically. Aging essentially ceased when  $T_g$  of the amorphous phase reached the aging temperature. The increase in matrix  $T_g$  and the reinforcing effect of the crystals produced a change in mechanical properties from elastomer-like to thermoplastic-like. © 2003 Elsevier Ltd. All rights reserved.

**Keywords:** Poly(lactide); Poly(lactide)/poly(ethylene glycol) blends; Aging

## 1. Introduction

In recent years, poly(lactic acid) (PLA) has attracted increasing attention as a candidate for use in disposables and biomedical applications [1–3]. The linear aliphatic thermoplastic polyester can be prepared either by catalytic ring opening polymerization of lactides (lactic acid dimers) or condensation polymerization of lactic acid monomers [1,2]. It has good physical properties such as high strength, thermoplasticity, and processability; and in a suitable disposal site it will degrade to natural products [4,5]. Lactic acid exists as two enantiomeric forms, the D(+) configuration and the naturally occurring L(–) configuration. These produce the corresponding enantiomeric polymers by conservation of the chiral center. Generally, commercial PLA grades are copolymers of L-lactide and D-lactide. The optical purity, defined as  $|L\% - D\%|$ , strongly affects the properties. Optically pure PLA is isotactic and highly

crystalline. Decreasing the optical purity reduces the degree of stereoregularity and crystallinity. Poly(L-lactide) with more than 15 mol% D-lactide is amorphous [6].

To date, PLA has been used mostly in the biomedical field as suture material, in orthopedic applications and for controlled drug delivery systems [7,8]. Applications of PLA in the packaging industry have been limited by low strain at break and high modulus. Attempts have been made to improve the mechanical properties, such as copolymerization of PLA with other monomers [9,10], blending with other polymers [3,11,12], and plasticization using biocompatible plasticizers [13,14,15]. It has been found that by copolymerizing PLA with other monomers, a wide range of mechanical properties can be achieved [9,10]. However, none of the copolymerization approaches is economically attractive for packaging applications. Blending PLA with various other polymers has been investigated, however only moderate improvement in mechanical properties was achieved [3,12].

Other efforts have focused on finding a plasticizer that will improve the mechanical properties of PLA. Candidates have included lactic acid monomer, poly(ethylene glycol)

\* Corresponding author. Tel.: +1-216-368-4186; fax: +1-216-368-6329.

E-mail address: [pah6@po.cwru.edu](mailto:pah6@po.cwru.edu) (A. Hiltner).

<sup>1</sup> Present address: PolyOne Corporation, Avon Lake, OH 44012, USA.

(PEG), glucosemonoesters, partial fatty acid esters, thermoplastic starch, and citrate ester [13–15]. Polyethylene glycol, the conventional name for poly(ethylene oxide) of low molecular weight ( $<20,000$ ), significantly improves elongation at break and softness of PLA. Miscibility of PLA/PEG blends has been studied extensively. It was found that blends with up to 30 wt% PEG were miscible when they were quenched from the melt. They exhibited a single  $T_g$  and had no detectable crystallinity of either constituent [14–17]. With higher PEG content, the PEG partially crystallized during cooling [16,17]. If the optical purity of the PLA were high enough, PLA also crystallized; however, PLA and PEG did not cocrystallize [18,19].

Although, PEG appeared to be an effective plasticizer for PLA, there was evidence that the blends were not stable, but experienced significant property changes over time. The glass transition temperature of the quenched blend with 30 wt% PEG was found to be about 10 °C, which suggested that this blend was rubbery at ambient temperature. However, tensile properties and dynamic mechanical properties measured after the blend had aged for a period of time indicated that it was glassy at ambient temperature [14,17,20]. The previous studies of PLA/PEG blends were carried out either immediately after the blend was prepared or after it had aged for a lengthy period of time [14,16,17,20]. None of the studies addressed the time-dependence of property changes or the mechanism of aging.

In the present work, the mechanism of long-term aging of PLA/PEG blends was studied with a PLA of low stereoregularity blended with up to 30 wt% PEG. Changes in solid state structure that occurred over time were correlated with changes in mechanical properties. Aging processes are often modulated by environmental effects [21–23], and for this reason the influence of relative humidity (RH) on aging of PLA/PEG blends was also considered.

## 2. Experimental

### 2.1. Materials

The study utilized a poly(lactic acid) (PLA) of low stereoregularity. The specific optical rotation,  $[\alpha]_D^{25}$ , of this PLA was  $-116$  as measured in chloroform at a concentration of  $1 \text{ g dl}^{-1}$  and 25 °C (Autopol III Polarimeter). From  $[\alpha]_D^{25}$ , the PLA was determined to have a D-lactide content of 13% by assuming  $[\alpha]_D^{25}$  of poly(L-lactide acid) and poly(D-lactide acid) to be  $-156$  and  $156$ , respectively [6]. The PLA exhibited 2 % crystallinity after annealing at 100 °C for 1000 min with melting temperature 132 °C, which was consistent with this level of stereoregularity [6]. The PLA had  $M_w = 160 \text{ kDa}$  and  $M_w/M_n = 1.6$  as determined by gel permeation chromatography (Perkin Elmer Series 200 GPC) using tetrahydrofuran with concentration of  $0.6 \text{ g dl}^{-1}$  at 40 °C and calibration to polystyrene

standards. The poly-(ethylene glycol) (PEG) had molecular weight 8000. The PEG was highly crystalline, even after quenching the crystallinity was about 95 % with melting temperature of 63 °C.

### 2.2. Methods

The polymers were vacuum dried overnight at 50 °C before processing. Melt-blends with compositions PLA/PEG 90/10, 85/15, 80/20 and 70/30 wt/wt were prepared using a counter-rotating twin screw extruder operating at 190 °C. To mold the blends into films 0.5 mm thick the pellets were sandwiched between Mylar® sheets and heated at 185 °C for 2 min with minimal pressure, for 2 min at 10 MPa pressure, for 6 pressure cycles between 10 and 0 MPa to remove air bubbles, for 2 min at 20 MPa, and quenched into ice water.

Blend films were stored under ambient conditions (23 °C, about 50% RH) to study the effects of aging. To study the effect of RH on aging, films were molded as described above but slowly cooled in the mold at about  $1 \text{ °C min}^{-1}$  and aged at ambient temperature in vacuum (0% RH).

Uniaxial stress–strain measurements were performed using an Instron model 1123 universal testing machine. Specimens were cut from the films according to ASTM 1708 micro-tensile specifications. The grip separation was 22.3 mm and the specimen width was 4.8 mm. Tests were carried out at a strain rate of  $50\% \text{ min}^{-1}$ . At least 2 specimens were tested for each condition. Engineering strain was calculated from the crosshead displacement. Engineering stress was defined conventionally as the force per initial unit cross-sectional area.

Differential scanning calorimetry (DSC) was carried out with a Perkin Elmer DSC-7. To obtain the thermal behavior of unaged materials, specimens weighing 5–10 mg were heated at 185 °C for 4 min in the DSC, quenched to  $-50 \text{ °C}$  at  $100 \text{ °C min}^{-1}$ , and heated to 185 °C at  $10 \text{ °C min}^{-1}$ . For the aging study, specimens were cut from molded films that had aged for various periods of time and thermograms were obtained with a heating rate  $10 \text{ °C min}^{-1}$ . Percent crystallinity was calculated using heats of fusion of 197 and  $94 \text{ J g}^{-1}$  for PEG [24] and PLA [6] crystals, respectively. The reported crystallinities are normalized to the weight fraction of the constituents in the blend.

Dynamic mechanical thermal analysis (DMTA) was performed on molded films with a DMTA MkII unit from Polymer Laboratories operating in the tensile mode. The relaxation spectrum was scanned from  $-60$  to  $80 \text{ °C}$  with a frequency of 1 Hz and a heating rate of  $3 \text{ °C min}^{-1}$ .

Thin sections were microtomed from the molded films at ambient temperature (Ultramicrotome MT6000-XL from RMC, Tucson, AZ, USA), placed between glass slides, and examined with transmission polarized light microscopy. Hot stage was used to heat up the sample for examination at elevated temperatures. Pictures were taken three minutes

after reaching desired temperatures. Atomic force microscopy (AFM) was performed on the microtomed surface or the free melt surface with a Nanoscope IIIa with MultiMode head and J-scanner. The tapping mode was used at ambient conditions. Commercial Si probes were chosen with a resonance frequency in the 300 kHz range. Height and phase images were recorded simultaneously. In phase images, higher modulus material appears brighter and the softer material appears darker.

### 3. Results and discussion

#### 3.1. Unaged PLA/PEG blends

Thermograms of quenched PLA and PLA/PEG blends showed no evidence for crystallization of either constituent. All the thermograms exhibited a single glass transition. Slowly cooling at  $10\text{ }^{\circ}\text{C min}^{-1}$  or even  $1\text{ }^{\circ}\text{C min}^{-1}$  also resulted in thermograms with a single glass transition, confirming that the blends were miscible. The  $T_g$  was taken as the midpoint of the inflection. Increasing PEG content of the blend caused the  $T_g$  to decrease from  $58\text{ }^{\circ}\text{C}$  for quenched PLA through ambient temperature to  $9\text{ }^{\circ}\text{C}$  for PLA/PEG 70/30 blend.

The dynamic mechanical relaxation behavior of the quenched blends is presented by the temperature dependence of loss tangent ( $\tan \delta$ ), storage modulus ( $E'$ ), and loss modulus ( $E''$ ) in Fig. 1. As in the DSC thermograms, a single glass transition was observed which gradually shifted through ambient temperature as PEG concentration increased. The peak temperature in  $\tan \delta$  was always about  $10\text{ }^{\circ}\text{C}$  higher than the  $T_g$  measured from DSC, whereas the peak temperature in  $E''$  correlated closely with  $T_g$  from DSC, Table 1. A large drop in  $E'$  accompanied the  $T_g$ . Due to the shift in  $T_g$  through ambient temperature, the value of  $E'$  at ambient temperature was two orders of magnitude lower for PLA/PEG 70/30 than for PLA.

The glass transition temperature of binary miscible blends is often expressed by the Fox equation [25]

$$\frac{1}{T_g} = \frac{w_1}{T_{g1}} + \frac{w_2}{T_{g2}} \quad (1)$$

where  $w$  is the weight fraction and the subscripts 1 and 2 refer to the blend constituents. The  $T_g$  of quenched PLA/PEG blends followed the empirical Fox equation, as shown

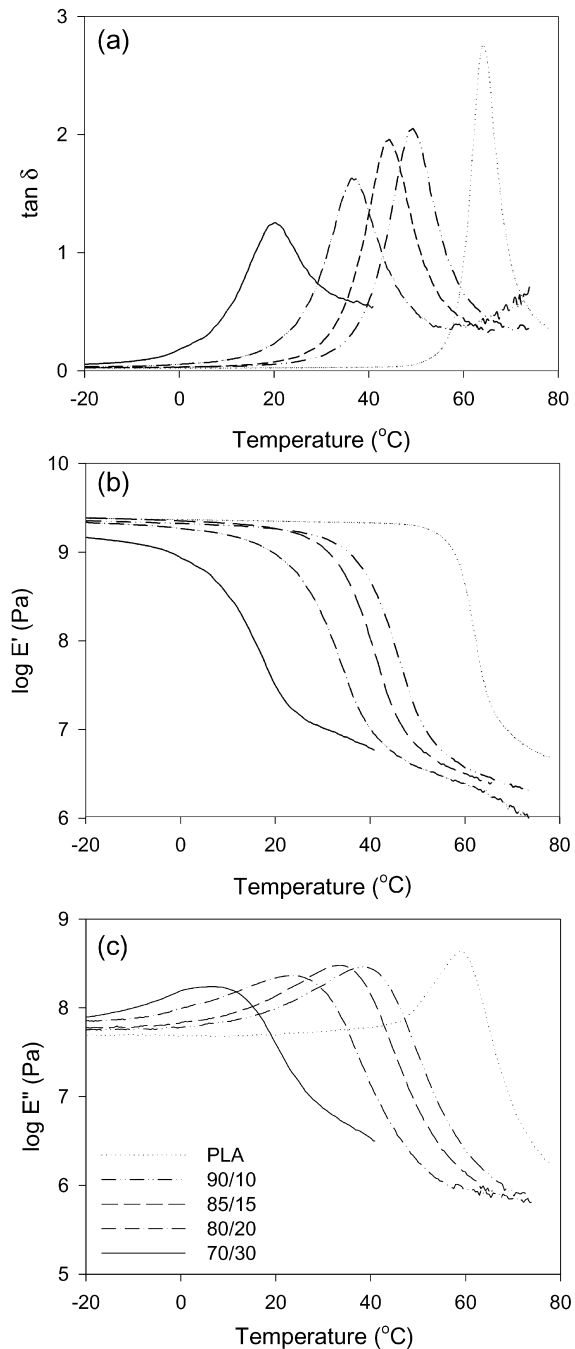


Fig. 1. Dynamic mechanical relaxation behavior of PLA and PLA/PEG blends: (a)  $\tan \delta$ ; (b)  $E'$ ; and (c)  $E''$ .

Table 1  
Effect of PEG content on the thermal and mechanical properties of quenched PLA/PEG blends

Composition PLA/PEG	$T_g$ from DSC ( $^{\circ}\text{C}$ )	$T_g$ from $E''$ ( $^{\circ}\text{C}$ )	2% secant modulus (MPa)	Yield stress (MPa)	Fracture strain (%)
100/0	58	59	$2200 \pm 50$	$53 \pm 2$	$14 \pm 1$
90/10	36	38	$950 \pm 30$	$23 \pm 1$	$200 \pm 10$
85/15	30	32	$630 \pm 20$	$16 \pm 1$	$260 \pm 10$
80/20	21	24	$180 \pm 20$	$5 \pm 1$	$300 \pm 20$
70/30	9	7	$5 \pm 1$	—	$500 \pm 20$

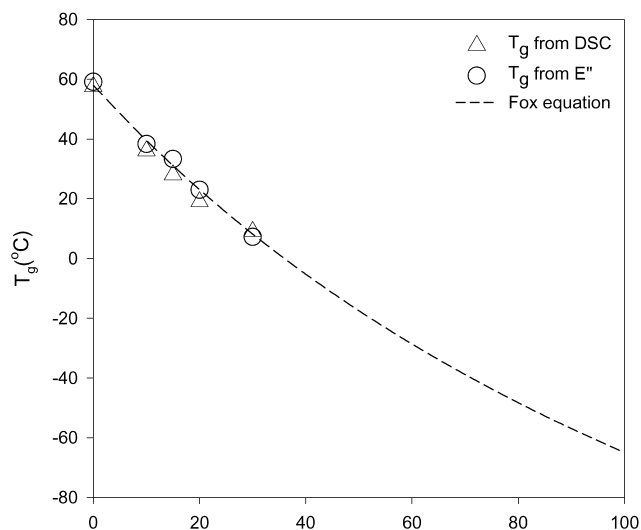


Fig. 2. Dependence of the glass transition temperature on blend composition.

in Fig. 2 where results from DSC and  $E''$  are plotted. The best solid line fit of the data was based on  $T_g$  of PEG of  $-66^\circ\text{C}$ . The  $T_g$  of PEG is reportedly in the range  $-55$  to  $-70^\circ\text{C}$  depending on molecular weight [16,20,26].

The stress–strain behavior of quenched PLA/PEG blends was examined at ambient temperature immediately after quenching, as shown in Fig. 3. Unmodified PLA was a stiff, relatively brittle polymer. It yielded with formation of an unstable neck that fractured after a short draw region. The yield stress was approximately 53 MPa and the fracture strain was 14%. Addition of 10% PEG improved the ductility dramatically, Table 1. The yield stress dropped to about 24 MPa and the fracture strain increased to nearly 200%. Blending with PEG significantly improved the softness of PLA and the elongation at break by decreasing the  $T_g$ . The 80/20 blend with  $T_g$  coincident with ambient temperature exhibited diffuse necking and complex yielding behavior. With  $T_g$  below ambient temperature, the modulus

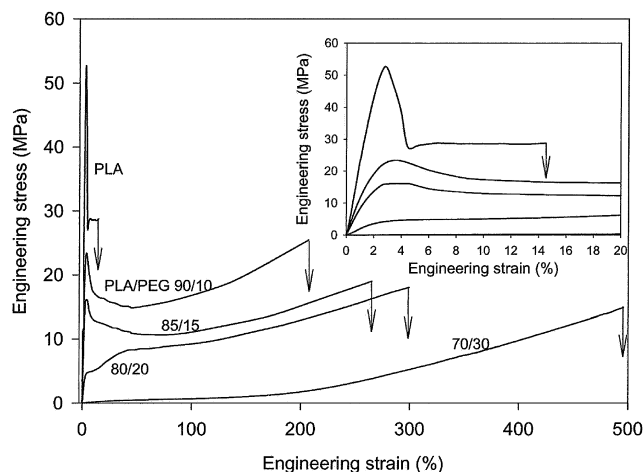


Fig. 3. Tensile stress–strain behavior of quenched PLA and PLA/PEG blends at ambient temperature. The insert shows the modulus and yielding regions on an expanded strain scale.

of the 70/30 blend decreased by two orders of magnitude compared to PLA and the elongation at break increased to 500%.

### 3.2. Aging of PLA/PEG 70/30 blends

Aging PLA/PEG 70/30 films under ambient conditions ( $23^\circ\text{C}$ , about 50%RH) produced the changes in tensile properties seen in Fig. 4. With time, the films changed from low modulus elastomer-like materials to higher modulus thermoplastic-like materials. After aging for 500 h the modulus increased almost two orders of magnitude and the fracture strain decreased from 500 to 250%, Table 2. After 500 h the aging process slowed down so that there was very little change in tensile properties between 500 and 1800 h.

Thermograms of aged PLA/PEG 70/30 are shown in Fig. 5. By itself PEG was highly crystallizable. Quenched PEG was about 95% crystalline with a melting temperature of  $63^\circ\text{C}$ . However PEG in the blends with PLA did not crystallize when the blend was quenched or slowly cooled from the melt. The thermogram of the 70/30 blend indicated that it was completely amorphous with a single  $T_g$  at  $9^\circ\text{C}$ . After aging for 2 h a small endothermic peak appeared at about  $58^\circ\text{C}$ , which corresponded to melting of PEG crystals. Upon further aging, the melting peak at  $58^\circ\text{C}$  became larger and a second endothermic peak developed at a slightly lower temperature, around  $46^\circ\text{C}$ . The  $58^\circ\text{C}$  peak was always much larger than the  $46^\circ\text{C}$  peak. Two melting peaks suggested that two types of PEG crystals formed during aging. In parallel with the appearance of PEG crystallinity, the baseline inflection that identified the glass transition broadened and shifted to higher temperature until it became too broad and too close to the PEG melting peak to be discerned. Aging times longer than 500 h resulted in minimal change in the thermogram.

The PLA used in this study was almost completely amorphous due to its low stereoregularity. A very small melting peak at  $132^\circ\text{C}$  in the DSC thermogram of PLA

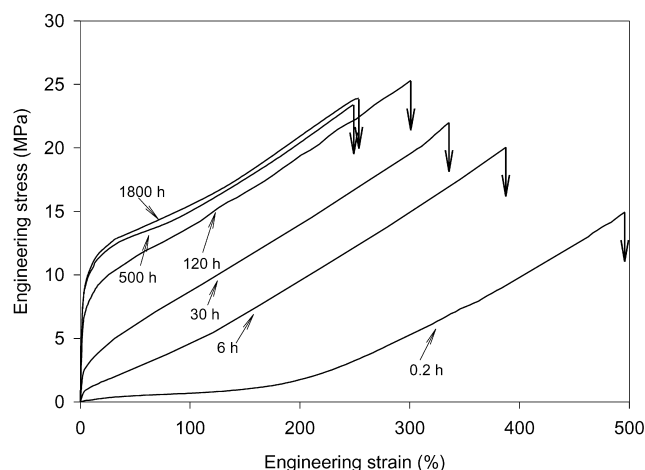


Fig. 4. Effect of aging under ambient conditions ( $23^\circ\text{C}$ , about 50% RH) on the tensile stress–strain behavior of the PLA/PEG 70/30 blend.

Table 2  
Effect of ambient aging on the thermal and mechanical properties of quenched PLA/PEG 70/30 blend

Aging time (h)	Crystallinity of PEG	Crystallinity of PLA	$T_g$ from $E''$ (°C)	2% secant modulus (MPa)	Yield stress (MPa)	Fracture strain (%)
0.2	0	0	7	$5 \pm 1$	–	$500 \pm 20$
2	0.03	0.01	N/A	$7 \pm 2$	–	$480 \pm 10$
6	0.05	0.02	N/A	$40 \pm 5$	$1 \pm 0.2$	$400 \pm 10$
30	0.08	0.03	14	$100 \pm 10$	$2 \pm 0.2$	$340 \pm 10$
75	0.16	0.04	N/A	N/A	N/A	N/A
120	0.35	0.09	N/A	$220 \pm 20$	$7 \pm 0.3$	$300 \pm 20$
500	0.60	0.12	22	$370 \pm 20$	$9 \pm 0.3$	$250 \pm 10$
1800	0.67	0.13	27	$400 \pm 20$	$9 \pm 0.3$	$240 \pm 20$
3200	0.68	0.14	N/A	N/A	N/A	N/A

annealed at 100 °C for 1000 min indicated that a small amount of crystallinity, estimated at about 2%, was attainable [6]. During aging of the 70/30 blend, a broad endotherm appeared at about 127 °C, which was attributed to melting of PLA crystals. The PLA crystallinity increased with aging time approximately in proportion to the PEG crystallinity, Table 2. At the longest aging time, the crystallinity of PLA was estimated from the melting enthalpy to be about 14% based on total PLA, which was considerably higher than the 2% crystallinity achieved by annealing PLA without PEG.

The increase in PEG crystallinity during aging is shown in Fig. 6. During the first 50 h the crystallinity increased very slowly on the logarithmic time axis, this was followed by a rapid increase between 50 and 500 h to a plateau at about 70% PEG crystallinity. The increase in 2% secant modulus during aging of the 70/30 blend is included in Fig. 6. The parallel dependencies of crystallinity and modulus on aging time confirmed that the changes in tensile properties were associated with crystallization of PEG.

Reducing the RH greatly retarded the rate of the aging process at ambient temperature. Thermograms of the 70/30 blend aged at 50 and 0% RH are compared in Fig. 7(a).

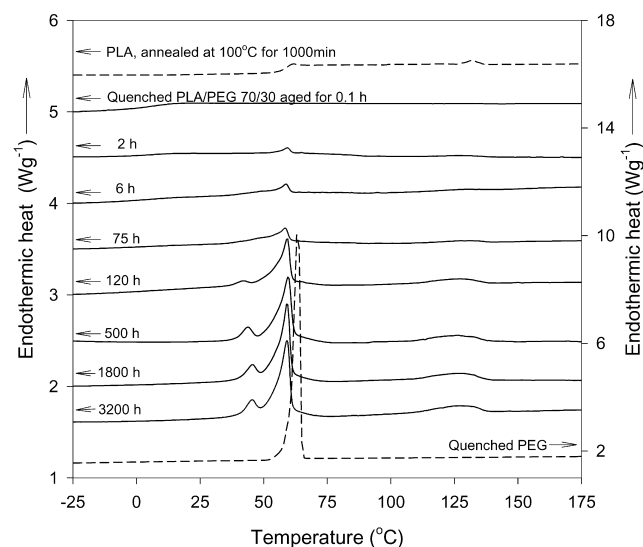


Fig. 5. Effect of aging under ambient conditions (23 °C, about 50% RH) on the thermogram of the PLA/PEG 70/30 blend.

Aging for 120 h at 0% RH resulted in only about 8% PEG crystallinity (2% PLA crystallinity) compared 35% PEG crystallinity after the same time at 50% RH. After 500 h at 0% RH the PEG crystallinity increased to 30% (6% PLA crystallinity), however this was still less than the 60% PEG crystallinity obtained in the same time at 50% RH. Although, aging at lower RH was slower, the thermograms of blends aged at 0 and 50% RH both exhibited a second small PEG melting peak and a broad PLA melting peak with enthalpy proportional to the PEG melting enthalpy. Similarity in these features suggested that the aging process at 0 and 50% RH was the same mechanistically, and differed only in rate. Aging at 0% RH also resulted in the same changes in tensile properties, although, the changes occurred more slowly than at 50% RH, Fig. 7(b). Increasing modulus and decreasing fracture strain reflected the level of crystallinity.

### 3.3. Crystallization during aging

Cross-sections of the quenched PLA/PEG 70/30 film were viewed in the polarized light microscope after the film had aged at 50% RH for various periods of time. After a short time, a small amount of birefringence appeared at the surface of the film, Fig. 8(a). The interior of the film was non-birefringent. After 75 h a few large spherulites

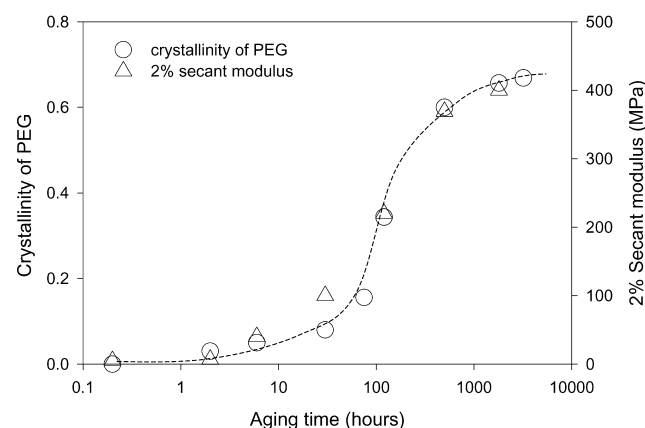


Fig. 6. Change in PEG crystallinity and 2% secant modulus of the PLA/PEG 70/30 blend with aging time.



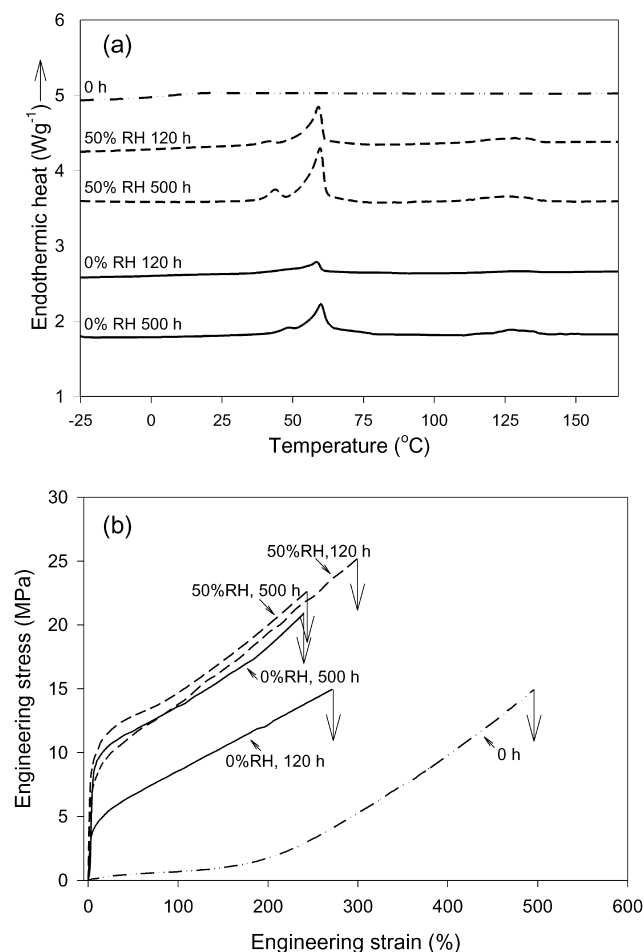


Fig. 7. Effect of RH on aging of PLA/PEG 70/30 at 23 °C: (a) thermograms; and (b) tensile stress–strain behavior.

appeared in the interior of the film, Fig. 8(b). The isolated spherulites were approximately the same size, about 70  $\mu\text{m}$  in diameter. At longer times, the spherulite density was much higher, after 1800 h the spherulites frequently impinged and approached space-filling, Fig. 8(c), however the spherulite size was relatively uniform and about the same as at the earlier time point. The combined observations suggested that nucleation was relatively slow, but once nucleated a spherulite grew rapidly until it reached a diameter on the order of 50–70  $\mu\text{m}$ . At this size growth ceased even though the spherulite might not impinge on other spherulites. With time spherulites nucleated at other locations and they gradually filled most of the remaining space. Thus increasing the aging time increased the spherulite density but did not increase the spherulite size.

The composition of the spherulites was probed by raising the temperature in the hot stage of the polarized light microscope through the melting points of PEG and PLA. A 70/30 blend film that was aged for 75 h is shown in Fig. 9 as it appears at various temperatures. No change was noticed between 23 and 55 °C. Between 55 and 65 °C, where PEG would melt, the spherulites lost most of their birefringence. Although, the spherulitic entities remained visible under

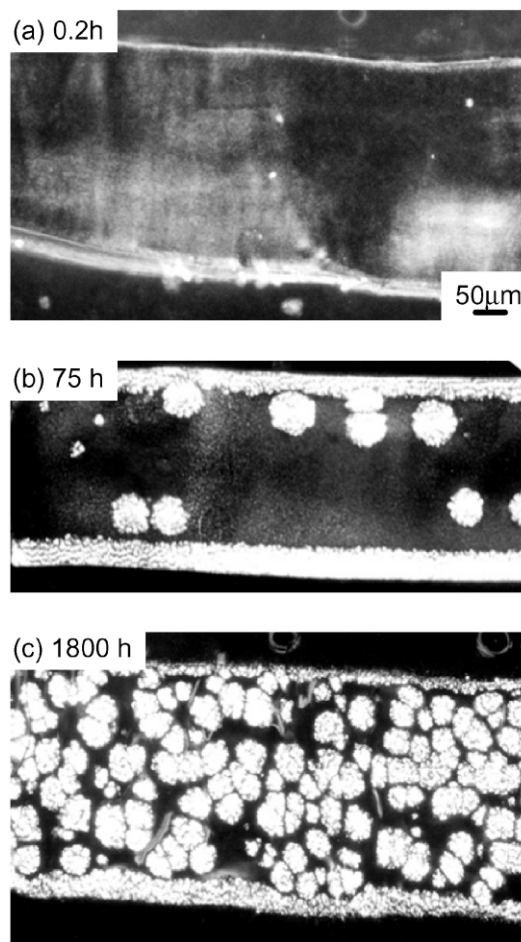


Fig. 8. Cross-sections of the PLA/PEG 70/30 blend as viewed in the polarizing light microscope after aging at ambient conditions for different periods of time.

polarized light, their highly reduced birefringence required much higher light intensity. The remaining birefringence disappeared between 120 and 135 °C, the melting range of PLA. It appeared that during aging PEG crystallized as spherulites. Some PLA that was trapped inside the spherulites also crystallized. It seems likely that PEG crystals nucleated crystallization of PLA within the spherulites. This was indicated by the absence of PLA birefringence in the matrix, by proportionality between PLA and PEG crystallinity, and by the high level of PLA crystallinity achieved in the blend relative to PLA without PEG.

The spherulitic morphology was probed with AFM images of the 70/30 blend. Immediately after quenching, or after aging for only a short time, the films were too soft to microtome at ambient temperature and too sensitive to water condensation to microtome at cryogenic temperature. The image in Fig. 10(a) shows a free surface of the quenched blend after it was aged for 1 h. There was no evidence of large crystalline entities at this early stage. The image in Fig. 10(b) from the interior of a film that was aged for 48 h shows a growing spherulite. The higher modulus

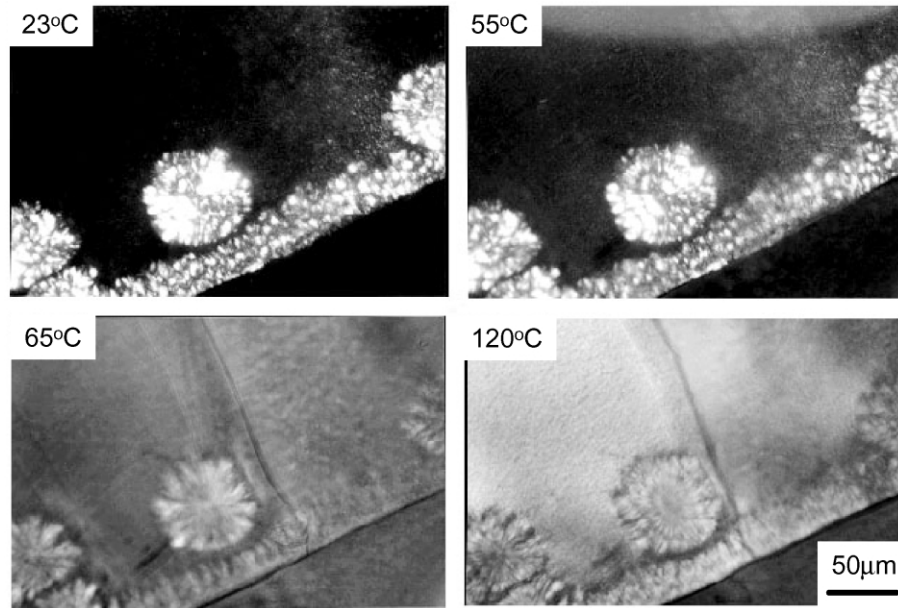


Fig. 9. Cross-section of the PLA/PEG 70/30 blend that was aged at ambient conditions for 75 h and viewed at various temperatures as it was heated on the hot-stage of the polarizing light microscope.

crystalline material appears brighter in the phase image and the softer amorphous matrix appears darker. The spherulite consisted of bright aggregates of crystals. It was not possible to differentiate PEG and PLA crystals. The crystalline aggregates were surrounded by a region of intermediate

brightness that extended about 2–3  $\mu\text{m}$  into the darker matrix.

More detail of the edge of the growing spherulite is seen in the higher resolution image in Fig. 10(c). The relative brightness of the various elements in the image suggests that

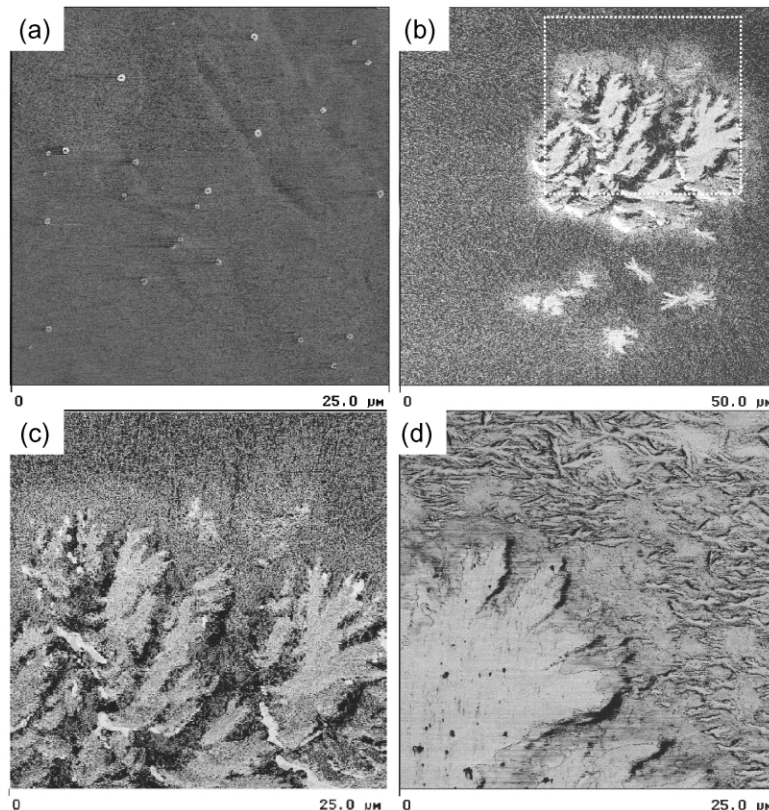


Fig. 10. AFM phase images of the PLA/PEG 70/30 blend after aging at ambient conditions for various periods of time: (a) free melt surface aged for 1 h; (b) microtomed surface after aging for 48 h; (c) higher resolution of (b); and (d) microtomed surface after aging for 480 h.

the crystalline aggregates were surrounded by a homogeneous region with modulus higher than the modulus of the non-crystalline matrix. The growing spherulite in Fig. 10(c) is compared with the edge of a fully grown spherulite that was obtained by aging for 480 h in Fig. 10(d). The diameter of the spherulite in Fig. 10(d) was about 70  $\mu\text{m}$ , the same size as the spherulites observed in the light microscope. The spaces between the crystalline aggregates had crystallized to create a solid crystalline mass that was surrounded by a featureless boundary layer with thickness 2–3  $\mu\text{m}$ . The matrix had acquired a texture that suggested additional small crystalline structures. These small structures might have produced the second PEG melting peak in DSC thermograms of the aged blend.

### 3.4. Model for aging of PLA/PEG blends

Although the  $T_g$  was not evident in DSC thermograms of aged films, dynamic mechanical relaxation measurements of the aged 70/30 blend showed peaks in  $\tan \delta$  and  $E''$  that corresponded to the glass transition, Fig. 11. As the blend aged the peak in  $\tan \delta$  decreased in intensity and broadened, and the peak temperature in  $\tan \delta$  and  $E''$  increased significantly, Table 2. However a single  $T_g$  was always observed in the aged blends, which indicated that the amorphous phase remained miscible during aging. Aging for 24 h increased  $T_g$  from 7 to 14  $^{\circ}\text{C}$  based on the peak in  $E''$ . Aging for 500 h increased the  $T_g$  by an additional 8 to 22  $^{\circ}\text{C}$  and aging for 1800 h increased it by an additional 5 to 27  $^{\circ}\text{C}$ . At this point, the  $T_g$  essentially coincided with the aging temperature.

It is suggested that the gradual increase in  $T_g$  was largely due to preferential crystallization of PEG, which depleted the amorphous regions of that constituent. To test this interpretation, the composition of the amorphous phase after aging was estimated. Assuming that non-crystallized PEG and PLA constituted the amorphous phase of the aged blend, the weight fraction of each constituent,  $W_{a,i}$ , in the amorphous phase after aging can be calculated as

$$W_{a,i} = \frac{W_i(1 - \phi_i)}{W_1(1 - \phi_1) + W_2(1 - \phi_2)} \quad (2)$$

where  $W_i$  is the weight fraction of the constituent in the unaged blend and  $\phi_i$  is the crystallinity of the constituent after aging. The composition of the amorphous phase after aging for 1800 h was determined to be about PLA/PEG 86/14. A homogeneous blend of this composition would have  $T_g$  of about 32  $^{\circ}\text{C}$  (Fig. 2), which was close to the observed  $T_g$  of 27  $^{\circ}\text{C}$  for the aged blend.

As  $T_g$  approached the aging temperature, reduced molecular diffusivity slowed the crystallization rate dramatically. After 1800 h at ambient temperature, the aging process had reached the plateau region (Fig. 6), and aging had essentially ceased before PEG had completely crystallized. At this point, about 67% of the PEG and about 13% of the PLA in the 70/30 blend was crystallized, although, PEG

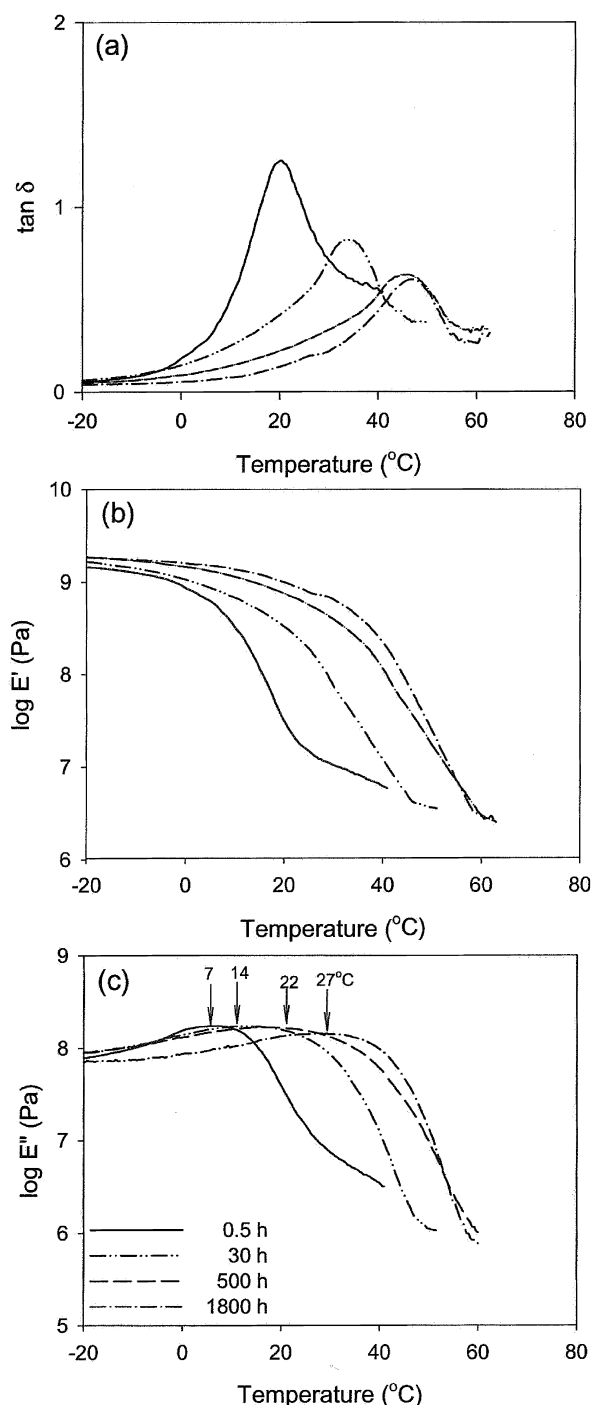


Fig. 11. Effect of aging on the dynamic mechanical relaxation behavior of PLA/PEG 70/30: (a)  $\tan \delta$ ; (b)  $E'$ ; and (c)  $E''$ .

can crystallize to a level of 95%. If indeed the onset of amorphous phase rigidity halted crystallization of PEG in the blend, PEG should crystallize further if the temperature is raised. This was confirmed when taking a 70/30 blend that had aged for several months at ambient conditions to 35  $^{\circ}\text{C}$  for 48 h increased the PEG crystallinity from 70 to 80%. Increasing the temperature further started to melt PEG crystals.

Crystallization of PEG significantly altered blend



mechanical properties. The change from low modulus elastomer-like behavior to higher modulus thermoplastic-like properties (Fig. 4) that accompanied aging reflected both the increasingly glassy nature of the matrix as  $T_g$  approached ambient temperature and the reinforcing effect of the spherulites as PEG and PLA crystallized.

No evidence was found for phase separation in the blends, indeed all the results indicated that PEG was miscible with PLA in compositions up to 30% PEG. In a miscible blend, crystal growth rate is a function of the glass transition temperature (chain mobility) and the equilibrium melting temperature relative to the crystallization temperature (degree of undercooling) [27–30]. Initially,  $T_g$  of the 70/30 blend was much lower than ambient temperature and PEG was able to crystallize. Crystallization of PEG depleted the surrounding amorphous region of PEG and locally increased  $T_g$ . This was evident in AFM phase images as a region of higher modulus than the bulk that surrounded the crystalline aggregates. As the modulus of the nearby amorphous material increased, diffusion of PEG to the growing spherulite slowed. The growth rate gradually decreased until growth essentially ceased when the local  $T_g$  reached the aging temperature. In this case, outward growth was halted by a large decrease in diffusion rate rather than by impingement on other spherulites. The effective limit on spherulite growth imposed by the local increase in  $T_g$  resulted in the characteristic uniformity of spherulite size. Further crystallization slowly filled-in the regions between crystalline aggregates of existing spherulites, while new spherulites nucleated and grew at other locations where the  $T_g$  was low and chains had high mobility. Due to the relatively low diffusion rate of the higher molecular weight PLA, some amount of PLA was trapped inside the PEG spherulites where its crystallization was probably nucleated by PEG crystals.

According to the aging model for PLA/PEG blends, the 80/20 blend with  $T_g$  just below ambient temperature was expected to exhibit some amount of aging, although, less than the 70/30 blend. Indeed, after 200 h the DSC thermogram indicated about 18% PEG crystallinity. The aging effect was confirmed by the DMTA curves (Fig. 12). After 500 h the peak temperature in  $E''$  increased from 23 to 28 °C. The  $\tan \delta$  peak also increased in temperature, broadened and decreased in intensity, and  $E'$  increased.

The 85/15 blend had  $T_g$  slightly above ambient temperature at 32 °C from  $E''$ . This composition exhibited almost no changes in the DMTA curves after aging for 300 h at ambient temperature, Fig. 13. However if the temperature was raised the 85/15 blend also underwent irreversible aging with crystallization of the PEG constituent. Amorphous PLA without PEG had  $T_g$  well above ambient temperature. It exhibited no changes after extended aging.

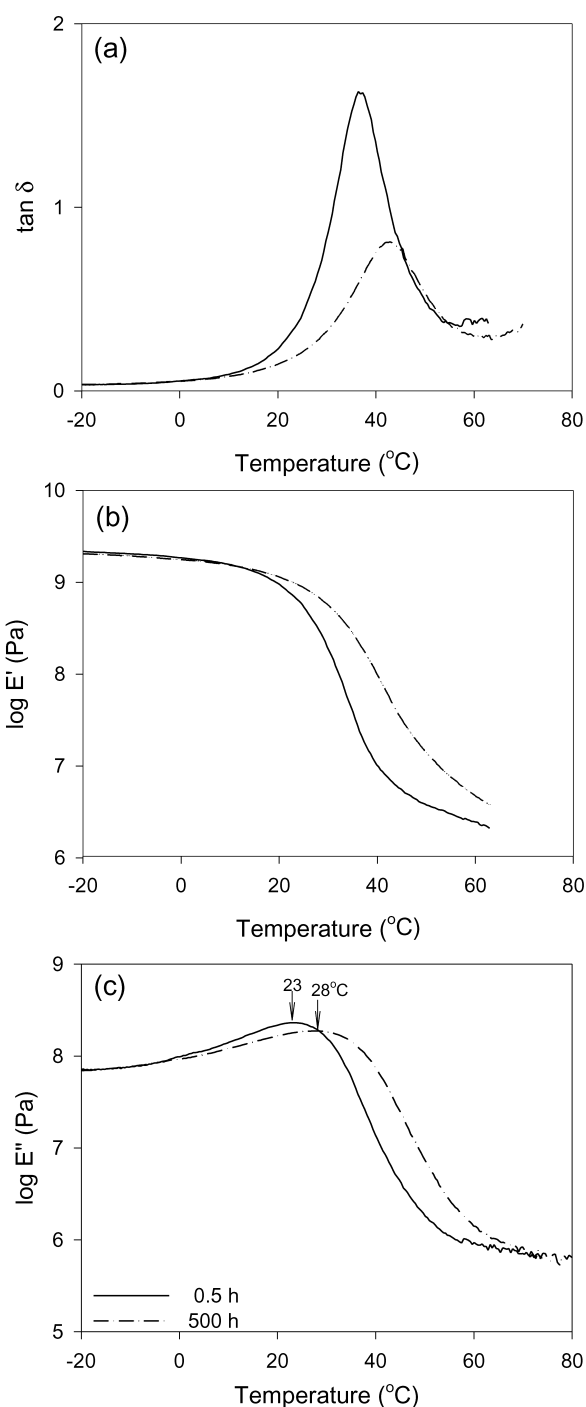


Fig. 12. Effect of aging on the dynamic mechanical relaxation behavior of PLA/PEG 80/20: (a)  $\tan \delta$ ; (b)  $E'$ ; and (c)  $E''$ .

#### 4. Conclusions

Addition of 30 wt% PEG to PLA of low stereoregularity decreased  $T_g$  from above ambient temperature to below ambient temperature and thereby decreased the modulus and increased the ductility of this relatively rigid, brittle thermoplastic. Immediately after cooling from the melt, blends with up to 30 wt% PEG were amorphous and homogeneous with a single  $T_g$  that depended on

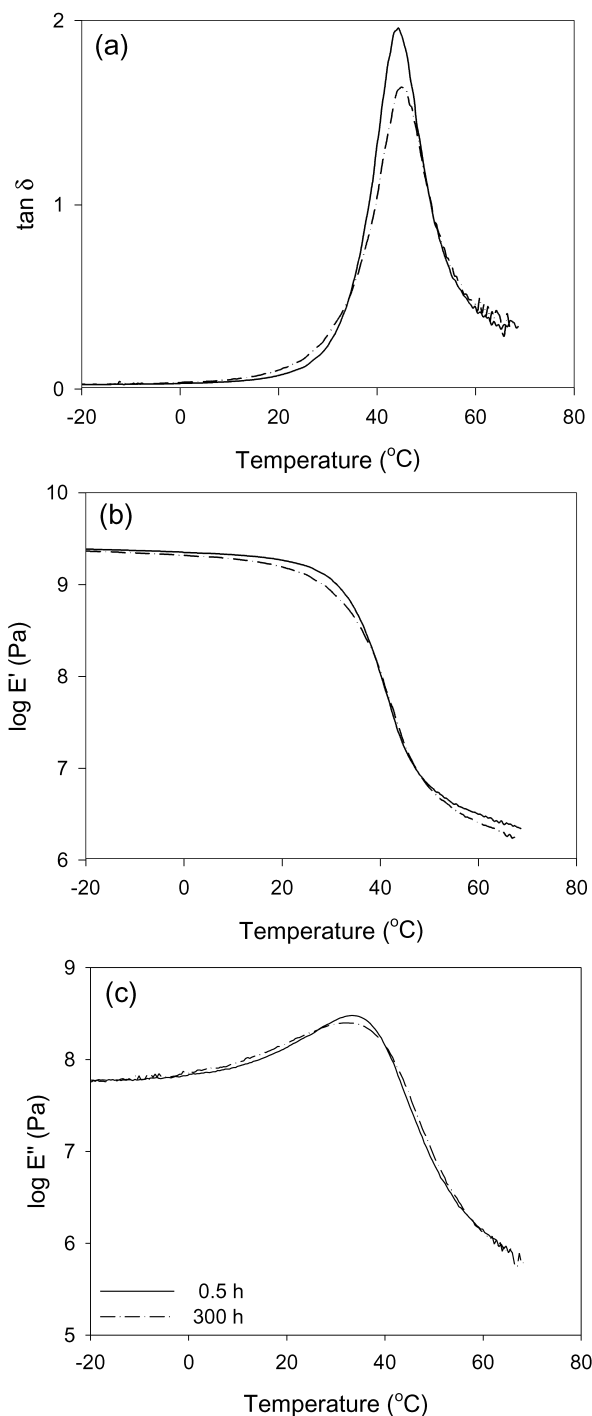


Fig. 13. Effect of aging on the dynamic mechanical relaxation behavior of PLA/PEG 85/15: (a)  $\tan \delta$ ; (b)  $E'$ ; and (c)  $E''$ .

composition in accordance with the Fox relationship. However, the blends with 20 wt% or more PEG were not stable at ambient temperature. Over time the modulus increased and the elongation at break decreased. The origin of the aging phenomenon was crystallization of PEG. Preferential crystallization of PEG gradually enriched the amorphous phase in PLA and increased  $T_g$  of the amorphous

phase. When  $T_g$  reached ambient temperature aging essentially ceased even though PEG was not completely crystallized. Reduced molecular diffusivity slowed the crystallization rate dramatically. Aging resumed if the temperature was raised above  $T_g$ . As a generalization, blends exhibited aging under ambient conditions if the PEG content was high enough to put  $T_g$  below ambient temperature. Conversely, the blend with 15 wt% PEG and  $T_g$  slightly above ambient temperature appeared to be stable over time under ambient conditions.

### Acknowledgements

The generous financial and technical support of the Kimberly-Clark Corporation is gratefully acknowledged.

### References

- [1] Dorgan J, Lehermeier J, Palade L, Cicero J. *Macromol Symp* 2001; 175:55.
- [2] Jscobsen S, Degee PH, Fritz HG, Dubois PH, Jerome R. *Polym Engng Sci* 1999;39:1311.
- [3] Grijpma DW, Van Hofslot R, Super H, Nijenhuis A, Pennings AJ. *Polym Engng Sci* 1994;34:1674.
- [4] Sinclair RG. *ANTEC* 1987;87:1214.
- [5] Kricheldorf HR, Kreiser-Saunders I. *Macromol Symp* 1996;103:85.
- [6] Tsuji H, Ikada Y. *Macromol Chem Phys* 1996;197:3483.
- [7] Bergsma JE, Bos RRM, Rozema FR, Jong WD, Boering G. *J Mater Sci, Mater Med* 1996;7:1.
- [8] Zhu KJ, Lin XZ, Yang SL. *J Appl Polym Sci* 1990;39:1.
- [9] Lee SY, Chin IJ, Jung JS. *Eur Polym J* 1999;35:2147.
- [10] Bechtold K, Hillmyer M, Tolman W. *Macromolecules* 2001;34:8641.
- [11] Meredith JC, Amis EJ. *Macromol Chem Phys* 2000;201:733.
- [12] Liu X, Dever M, Fair N, Benson R. *J Environ Polym Degrad* 1997;5: 225.
- [13] Jacobsen S, Fritz HG. *Polym Engng Sci* 1999;39:1303.
- [14] Martin O, Averous L. *Polymer* 2001;42:6209.
- [15] Ljungberg N, Wesslen B. *J Appl Polym Sci* 2002;86:1227.
- [16] Yang JM, Chen HL, You JW, Hwang JC. *Polym J* 1997;29:657.
- [17] Nijenhuis A, Colstee E, Grijpma DW, Pennings AJ. *Polymer* 1996;37: 5849.
- [18] Nakafuku C, Sakoda M. *Polym J* 1993;25:909.
- [19] Younes H, Cohn D. *Eur Polym J* 1988;24:765.
- [20] Sheth M, Kumar BA, Dave V, Gross RA, McCarthy SP. *J Appl Polym Sci* 1997;66:1495.
- [21] Sheldon RP. *Polymer* 1962;3:27.
- [22] Cornelis H, Kander RG, Martin JP. *Polymer* 1996;37:4573.
- [23] Tashiro K, Ueno Y, Yoshioka A, Kobayashi M. *Macromolecules* 2001;34:310.
- [24] Campbell C, Viras K, Richardson MJ, Masters AJ, Booth C. *Makromol Chem* 1993;194:799.
- [25] Olabisi O, Mobeson LM, Shaw MT. *Polymer-polymer miscibility*. New York: Academic Press; 1979.
- [26] Faucher JA, Koleske JV, Santee ER, Stratta JJ, Wilson CW. *J Appl Phys* 1966;37:3962.
- [27] Runt PJ. In: Paul DR, Bucknall CB, editors. *Polymer blends*, Vol. 1. New York: Wiley; 2000. Chapter 6.
- [28] Shabana HM, Olley RH, Bassett DC, Jungnickel BJ. *Polymer* 2000; 41:5513.
- [29] Dreezen G, Fang Z, Groeninckx G. *Polymer* 1999;40:5907.
- [30] Hsiao BS, Sauer BB. *J Polym Sci, Polym Phys Ed* 1993;31:901.